

SYNTHESIS AND CHARACTERIZATION OF Fe₃O₄ NANOPOWDER AND DIELECTRIC STUDIES

V. Maria Vinosel, A. PersisAmaliya, S. Vijayalakshmi, S.Pauline

Department of Physics, Loyola College, University of Madras, Chennai – 34, India

*Corresponding author: vinovincent90@gmail.com

Abstract— Iron oxide (Fe₃O₄) nanoparticles were synthesized by hydrothermal method. The chemical composition and morphologies of the as-prepared samples were characterized by X-ray diffraction (XRD), Fourier transform infrared spectra (FTIR), Scanning Electron microscopy (SEM) and Energy dispersive X-ray analysis (EDAX). XRD confirms the presence of pure cubic phase Fe₃O₄ without any impurities. SEM image indicates the formation of agglomerated nanospheres. FTIR confirms the presence of metal-oxygen bond. The dielectric studies are also reported.

Index terms- Fe₃O₄; XRD; FTIR; SEM; Dielectric studies..

I. INTRODUCTION

Fe₃O₄ is known as black iron oxide or magnetic oxide material. Magnetite, Fe₃O₄ is a ferrimagnetic mineral belonging to the family of inverse spinels[1]. Maghemite is another kind of iron oxide that has the same crystalline structure as Fe₃O₄. There are various phases of iron oxides namely goethite (α -FeOOH), maghemite (γ -Fe₂O₃), magnetite (Fe₃O₄) and hematite (α -Fe₂O₃). The most commonly used magnetic materials are magnetite (Fe₃O₄) and maghemite (γ -Fe₂O₃) for bioapplications. Super-paramagnetic behavior of magnetic nanoparticles is desired for biomedical applications in order to avoid agglomeration[2-3]. Magnetic nanoparticles are widely used in the field of magnetic resonance imaging (MRI), tissue repair, bioseparation, hyperthermia, targeted drug delivery, data storage, ferrofluids, and catalysis [4]. Several techniques have been used to prepare Fe₃O₄ nanoparticles, namely hydrothermal process, co-precipitation, microemulsion, sol-gel, and chemical reduction methods. Most of these methods are used to prepare the iron oxides with different dimensions such as zero dimensional quantum dots; one dimensional wire, rods, and tubes; two dimensional rings, disks, and sheets; and three dimensional hollow spheres [1]. When the particle size is reduced from micro scale to nano scale, they have electrical, optical, or magnetic properties that mostly differ from their bulk counterpart [5]. In the current study, a simple hydrothermal process for the synthesis of Fe₃O₄ nanoparticle is reported. The synthesis was surfactant less, simple, inexpensive, and highly repeatable [6].

II. EXPERIMENTAL

All the chemicals were of analytical grade. In a typical procedure, 2M of FeCl₂ was dissolved in 20 ml of distilled water to form a homogeneous solution. Then, 4M of NaOH was dissolved in 20 ml of distilled water. The aqueous solution of NaOH was rapidly poured into the above solution under vigorous stirring. The whole mixture was stirred for 20 min at room temperature. Then the solution was transferred in to a 50 ml of Teflon sealed autoclave for hydrothermal treatment at 180°C for 12h. After the reaction autoclave was allowed to cool down to room temperature. The resulting product was washed several times with distilled water and ethanol by centrifugation. The final product was dried at 50°C for 12h.

III. RESULT AND DISCUSSION

A. X-ray diffraction (XRD) analysis

The XRD pattern of the as synthesized Fe₃O₄ is shown in fig.1 All diffraction peaks were indexed to the cubic inverse spinel structure of Fe₃O₄ similar to that of the bulk Fe₃O₄ (ICDD card number 85-1436[7]), with a lattice constant a=b=c=8.381 Å. Wang et al. [8] have reported a one-step hydrothermal process to prepare highly crystalline Fe₃O₄ nanopowders without using the surfactants.

The average crystallite size of Fe₃O₄ nanoparticles were calculated from the major (311) diffraction peak using Debye Scherrer formula. The crystallite size of Fe₃O₄ nanoparticles was found to be 30 nm.

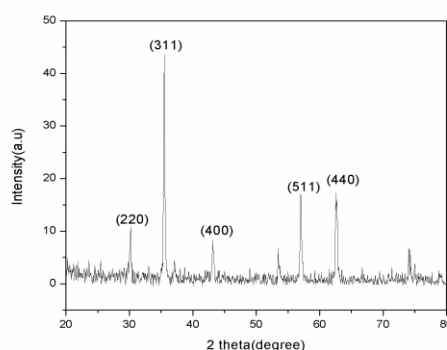


Fig.1 XRD spectrum of Fe_3O_4 nanoparticles

B. Fourier Transform Infrared (FT-IR) Analysis

The FTIR transmission spectra of Fe_3O_4 nanoparticles are shown in fig 2. The absorption band at 584 cm^{-1} is assigned to Fe-O stretching vibration mode. The values of the peaks at 796 cm^{-1} and 864 cm^{-1} are assigned to Fe-O-H bending vibration in $\alpha\text{-FeOOH}$ and these IR bands are generally used for the identification of $\alpha\text{-FeOOH}$ in phase analysis, respectively. The band obtained at 1571 cm^{-1} may correspond to asymmetrical H-O-H. The band observed at 3416 cm^{-1} is attributed to hydroxyl group.

N.D Kandpal et al. [9] have reported similar absorption and IR peaks were absorbed in the synthesis of Fe_3O_4 . These results are also in confirmation with the reports of [Wensheng Luet al \[10\]](#) Fe_3O_4 nanoparticles.

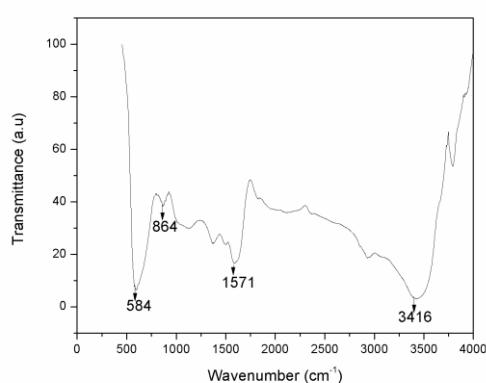


Fig.2. FTIR spectrum of Fe_3O_4 nanoparticles

C. Scanning electron microscopy (SEM) studies

A. Manikandan et al. [11] reported the morphology of Fe_3O_4 synthesized by microwave method to be nanospheres. Using Scanning electron microscope the surface structure of the as prepared sample was probed. Fig 3 shows SEM image for different magnification Fe_3O_4 nanoparticles appear to be nanospheres and homogenous in size distribution with strong agglomeration. SEM images demonstrated the high yield of Fe_3O_4 nanospheres obtained from the surfactant less synthetic route.

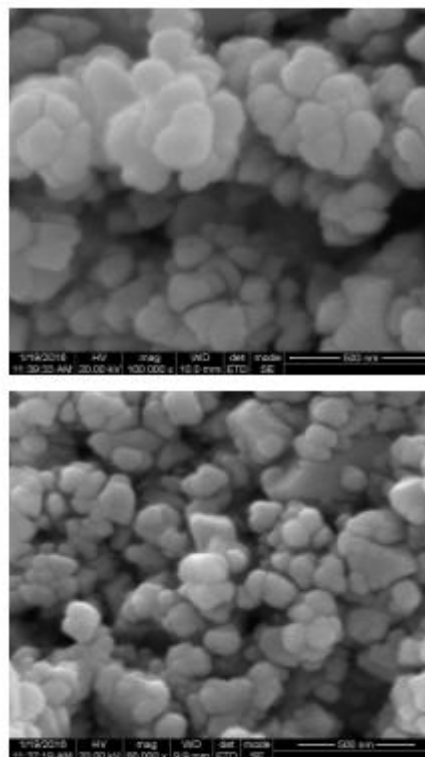


Fig.3. SEM micrograph of Fe_3O_4 nanoparticles

D. Energy dispersive X-ray (EDX) analysis

Energy dispersive X-ray (EDX) spectra revealed the presence of stoichiometric proportion of Fe and O elements without extra signals. This confirms the pure phase of Iron oxide.

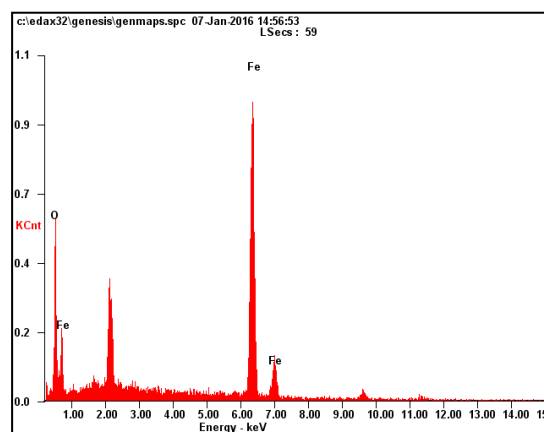


Fig.4 EDX analysis of Fe_3O_4 nanoparticles

E. Dielectric Studies

The dielectric constant of the Fe_3O_4 pellet was measured using HIOKI 3532LCR Hi TESTER in the frequency range from 50 Hz to 5 MHz. The samples were mounted between the two electrodes. The capacitance of the parallel plate capacitor formed by the electrodes, with the sample as a dielectric medium was measured. The variation of capacitance was

recorded in the frequency range 50Hz to 5MHz at different temperatures. The dielectric constant of the material was calculated for different frequencies from the measured capacitance values. The plot of the dielectric constant versus $\log f$ is shown in fig 5. It is observed that the dielectric constant has high value in the low frequency region and thereafter decreases with the applied frequency. The high value of ϵ' at low frequencies may be due to the presence of all the four polarizations namely space charge, orientation and, electronic and ionic polarization and the low values at higher frequencies may be due to the loss of significance of these polarizations gradually. The variation of dielectric loss with frequency is shown in fig 6. The AC electrical conductivity was determined using the relation $\sigma_{ac} = \omega \epsilon_0 \epsilon_r \tan \delta$ ($\omega = 2\pi f$, f is the frequency). With the high AC resistance it can be mentioned that the space charge polarization plays an important role in the electrical property of the sample and it was depicted in Fig 7

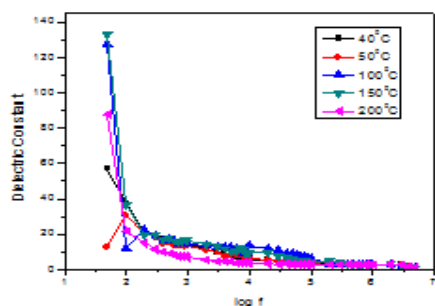


Fig.5 variation of dielectric constant vs $\log f$

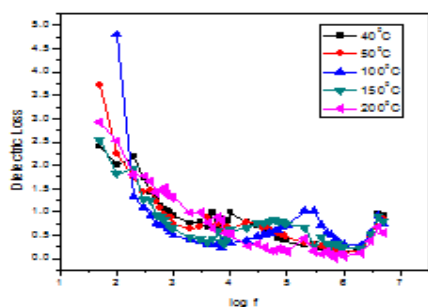


Fig.6 variation of dielectric loss vs $\log f$

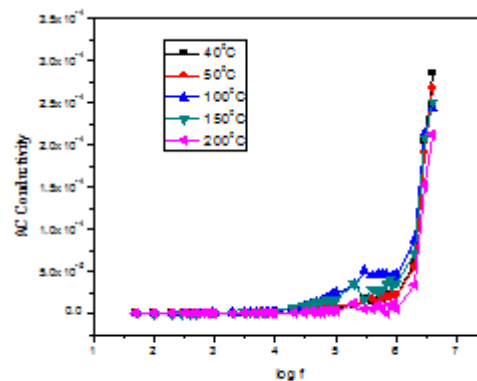


Fig.7 variation of AC conductivity vs $\log f$

IV. CONCLUSION

In summary, Fe_3O_4 nanoparticles were synthesized by hydrothermal method. The X-ray diffraction confirms the pure cubic phase of Fe_3O_4 . The FTIR spectra of Fe_3O_4 nanoparticles at 584 cm^{-1} is for Fe-O stretching vibration mode. SEM indicates the formation of agglomerated nanospheres. The dielectric constant decreases continuously at lower frequencies and remains constant at higher frequencies. Further work can be done on the relationship between size and electrochemical properties of the nanostructured Fe_3O_4 . For further analysis VSM studies can be used to confirm the magnetic property of the material.

REFERENCES

- Roychowdhury, S.P. Pati, A.K. Mishra, S. Kumar, D. Das, J. Phys. Chem. Solids 74 (2013) 811.
- Manish K. Sinha, Sushanta K. Sahu, Pratima Meshram, L.B. Prasad, Banshi D. Pandey Powder Technology 276 (2015) 214–221.
- B.D. Cullity, C.D. Graham, Introduction to Magnetic Materials, second ed., John & Wiley Sons, USA, 2009.
- R. Hiergeist, W. Andra, N. Buske, R. Hergt, I. Hilger, U. Richter, W. Kaiser, J. Magn. Magn. Mater. 201 (1999) 420.
- C. Buzea, I. Pacheco, and K. Robbie, "Nanomaterials and nanoparticles: sources and toxicity," *biointerphases*, 2007.
- Zhipeng Cheng, XiaoZhong Chu, Jingzhou Yin, HuiZhong, JimingXu Materials Letters 75 (2012) 172–174.
- R. Chen, J. Cheng, Yu Wei, J. Alloys Compd. 520 (2012) 266.
- J. Wang, J. Sun, Q. Sun, Q. Chen, Mater. Res. Bull. 38, 1113 (2003).
- N D Kandpal, N sah, R Loshah, R Joshi, and J Prasad Journal of scientific & Industrial research vol.73 February 2014, PP.87-90
- W. Lu, Y. Shen, A. Xie, W. Zhang, Green, J. Magn. Magn. Mater. 322 (2010) 1828–1833.
- A. Manikandan, J. Judith Vijaya, J. Arul Mary, L. John Kennedy, A. Dinesh Journal of Industrial and Engineering Chemistry 20 (2014) 2077–2085.